

Received 8 July 2016

Accepted 1 November 2016

Edited by N. B. Bolotina, Russian Academy of Sciences, Russia

Keywords: fluoroelpasolites; ammonium; dynamic orientational disorder; electron-density profiles; vibrational spectra.**CCDC references:** 1514174; 1514175**Supporting information:** this article has supporting information at journals.iucr.org/b

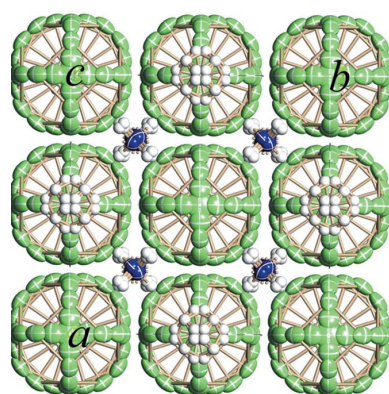
Crystallographic features of ammonium fluoro-elpasolites: dynamic orientational disorder in crystals of $(\text{NH}_4)_3\text{HfF}_7$ and $(\text{NH}_4)_3\text{Ti}(\text{O}_2)\text{F}_5$

Anatoly A. Udoenko,^{a*} Alexander A. Karabtsov^b and Natalia M. Laptash^a^aInstitute of Chemistry, Far Eastern Branch of RAS, Pr. Stoletiya 159, Vladivostok 690022, Russian Federation, and ^bFar Eastern Geological Institute, Far Eastern Branch of RAS, Pr. Stoletiya 159, Vladivostok 690022, Russian Federation.^{*}Correspondence e-mail: udoenko@ich.dvo.ru

A classical elpasolite-type structure is considered with respect to dynamically disordered ammonium fluoro-(oxofluoro-)metallates. Single-crystal X-ray diffraction data from high quality $(\text{NH}_4)_3\text{HfF}_7$ and $(\text{NH}_4)_3\text{Ti}(\text{O}_2)\text{F}_5$ samples enabled the refinement of the ligand and cationic positions in the cubic $Fm\bar{3}m$ ($Z = 4$) structure. Electron-density atomic profiles show that the ligand atoms are distributed in a mixed (split) position instead of $24e$. One of the ammonium groups is disordered near $8c$ so that its central atom (N1) forms a tetrahedron with vertexes in $32f$. However, a center of another group (N2) remains in the $4b$ site, whereas its H atoms (H2) occupy the $96k$ positions instead of $24e$ and, together with the H3 atom in the $32f$ position, they form eight spatial orientations of the ammonium group. It is a common feature of all ammonium fluoroelpasolites with orientational disorder of structural units of a dynamic nature.

1. Introduction

There is a large family of A_2BMX_6 compounds (A, B = alkali cations or ammonium, $R_A > R_B$; M = tri-, tetra-, penta- or hexavalent metal; X = O, F) with an elpasolite structure derived from a perovskite superstructure with doubled cell parameter (Massa & Babel, 1988; Flerov *et al.*, 1998). Named after the mineral K_2NaAlF_6 , elpasolite-type compounds are cubic face-centered with $Fm\bar{3}m$ space group ($Z = 4$; Morss, 1974). In this structure of A_2BMX_6 , B ions locate in the octahedral $4b$ sites surrounded by six F^- ligands, each of them belonging to a different MF_6^{3-} anion, and A ions are located in the tetrahedral $8c$ sites surrounded by 12F^- ions, each three of them belonging to one of the four MF_6^{3-} ions around the A ion. Precision structural determination of the Rb analogue of the mineral elpasolite, synthetic $\text{Rb}_2\text{NaAlF}_6$, was recently performed (Yakubovich *et al.*, 2013) in the classic style with $4a$, $4b$, $8c$ and $24e$ positions of the $Fm\bar{3}m$ group for Al, Na, Rb and F atoms, respectively. Most of the structures of cubic elpasolites were solved in a similar way. Nevertheless, the use of a classical $24e$ ligand position is not able to explain some structural transformations at phase transitions (PTs) inherent to cubic elpasolites. Recently, a synchrotron powder diffraction study of a synthetic cryolite Na_3AlF_6 revealed that the high-temperature (HT) cubic phase was characterized by static displacive disorder of the F anions from the $24e$ sites to four nearby $96k$ sites 25% occupied (Zhou & Kennedy, 2004). However, a simple static displacement of the F atoms is not capable of explaining the structure of the high-temperature β phase (Smrčok *et al.*, 2009). Relatively frequent reorientations of the AlF_6 octahedra of the β phase explain the thermal



© 2017 International Union of Crystallography

disorder in positions of the F^- ions observed in X-ray diffraction experiments (Bučko & Šimko, 2016). The dynamic nature of the β phase was confirmed by the entropy value (close to $Rln4$) during a first-order phase transition from monoclinic (α phase) symmetry (Yang *et al.*, 1993). The $96k$ position was taken into consideration to refine a cubic structure of Rb_2KFeF_6 (Vasilovsky *et al.*, 2006), while Massa *et al.* (1986) used the $96j$ position. The compound undergoes a PT at 170 K with the entropy change $\Delta S = Rln6$. A PT in the related Rb_2KTiOF_5 at 215 K is accompanied by quite a large change in the entropy, $\Delta S = Rln8$ (Fokina *et al.*, 2008; Gorev *et al.*, 2010), which is characteristic of order-disorder transformations as opposed to displacive ones associated with small octahedral tilts and followed by a rather small entropy change, which is of the order of $0.2R$ (Flerov *et al.*, 1998, 2002, 2004).

The PT entropy changes should be taken into account to refine the structures of elpasolites. It especially concerns ammonium fluoroelpasolites, which are usually dynamically disordered. Suga and co-authors (Moriya *et al.*, 1977, 1979; Kobayashi *et al.*, 1985; Tressaud *et al.*, 1986) measured the heat capacity of $(NH_4)_3MF_6$ ($M = Fe, Al, V, Cr, Ga$) and interpreted the observed large entropy changes of the phase transition in terms of a model in which the disordered orientations of the tetrahedral NH_4 ions at the $4b$ sites and of the octahedral MF_6^{3-} ions in the $Fm\bar{3}m$ lattice freeze into an ordered state below the transition points. Fluorine octahedra were assumed to be disordered with eight possible orientations in the general $192l$ position, and one of the ammonium ions at the $4b$ site was disordered in two distinct orientations. The total entropy change connected with both octahedra and tetrahedra ordering could be given as $\Delta S = Rln8 + Rln2 = Rln16$, which is in good agreement with the experimental values. However, the NH_4 group in the $8c$ position can also take part in the PT. PTs and ionic motions in hexafluoroaluminates $(NH_4)_{3-x}K_xAlF_6$ ($x = 1, 2$) studied by 1H , ^{19}F and ^{27}Al magnetic resonance were interpreted in terms of overall reorientations of NH_4^+ ($8c$ position) and AlF_6^{3-} ions. Rapid reorientations of both ions freeze into an ordered state below the PT points (Hirokawa & Furukawa, 1988). A recent study of the $(NH_4)_3GaF_6$ structure by ^{19}F and $^{69,71}Ga$ magic angle spinning NMR in comparison with X-ray Rietveld refinement supported the model of rigid GaF_6 octahedra. In spite of the very low deviation of the GaF_6 octahedra from exact cubic symmetry, it was concluded that the fluorine $192l$ position was much subjected to errors. Both NH_4^+ ions and GaF_6^{3-} octahedra undergo rapid reorientation rotations (Krahl *et al.*, 2008).

Our structural refinement of a series of ammonium fluoroelpasolites $(NH_4)_3AlF_6$, $(NH_4)_3TiOF_5$, $(NH_4)_3FeF_6$ and $(NH_4)_3WO_3F_3$ by localizing anions (F^- , O^{2-}) in four acceptable positions of the $Fm\bar{3}m$ system ($24e$, $96k$, $24e + 96j$, $192l$) revealed that F (O) atoms should be preferably distributed in mixed (split) $24e + 96j$ positions (Udovenko *et al.*, 2003). The same concerns $(NH_4)_3MoO_3F_3$ and seven-coordinated $(NH_4)_3ZrF_7$ and $(NH_4)_3NbOF_6$ (Udovenko & Laptash, 2008a, 2008b). Both ammonium groups are disordered: $N1H_4$ is tetrahedrally displaced from the $8c$ position into the $32f$ site, and the H atoms of $N2H_4$ are statistically distributed in the

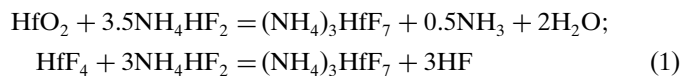
$96k$ and $32f$ positions, so that it takes eight equivalent spatial orientations instead of two accepted ones (Udovenko & Laptash, 2011). This disorder has a dynamic nature (both ammonium cations and anions are disordered) that was supported by solid-state NMR (Kavun *et al.*, 2010; 2011) and calorimetric measurements (Flerov *et al.*, 2011; Fokina *et al.*, 2007, 2013). This concerns equally both six-coordinated and seven-coordinated complexes.

Seven ligand atoms around a central metal atom lead with the need to the splitting of the ligand positions as in the case of ammonium fluoroperoxoelpasolites $(NH_4)_3Ti(O_2)F_5$ and $(NH_4)_3Zr(O_2)F_5$ (Massa & Pausewang, 1978; Schmidt *et al.*, 1986). In this paper, the crystallographic features of ammonium fluoroelpasolite structures are highlighted by examples of the dynamically disordered $(NH_4)_3HfF_7$ and $(NH_4)_3Ti(O_2)F_5$.

2. Experimental

2.1. Synthesis

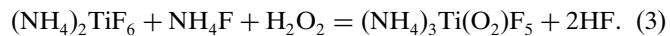
All the starting materials were of analytical reagent grade and used without further purification; deionized water was used as a solvent. Either solid NH_4HF_2 or hydrofluoric acid (40% HF by weight) were used as fluorinating agents. Ammonium hafnium fluoroelpasolite $(NH_4)_3HfF_7$ (I) was synthesized according to the reactions



Excess NH_4HF_2 or $(HF + NH_3)$ is needed to obtain the complex; we used a double excess. In the first case, HfO_2 or HfF_4 were fluorinated with NH_4HF_2 at 423–473 K followed by water leaching of the cake with the addition of a small amount of HF to pH = 2–3. The solution was filtered and slowly evaporated in air at ambient conditions with the formation of well faceted colorless octahedral single crystals of $(NH_4)_3HfF_7$. In the second case, HfO_2 was dissolved in the HF solution (40%) followed by the addition of NH_3 aq (25%) and slow evaporation of the resulting solution.

An attempt was made to obtain $(NH_4)_3HfOF_5$ by ammonia hydrolysis of the hot aqueous solution of $(NH_4)_3HfF_7$ with excess NH_4F , similar to $(NH_4)_3TiOF_5$ (Laptash *et al.*, 1999). At pH = 8 a white precipitate was formed (not identified) but $(NH_4)_3HfF_7$ crystallized again from the mother liquor. EDX analysis was used to check the composition of the crystal, which corresponded to $(NH_4)_3Hf(OH)_xF_7-x$ ($x = 0.2–0.4$).

Ammonium titanium peroxofluoroelpasolite $(NH_4)_3Ti(O_2)F_5$ (II) was prepared by synthesis from fluoride solution according to the reaction



An excess (50–100% with respect to the stoichiometric proportion) of NH_4F (40% solution) and then a concentrated (30%) solution of H_2O_2 were added to aqueous $(NH_4)_2TiF_6$

Table 1

Crystal and experimental data for $(\text{NH}_4)_3\text{HfF}_7$ (I) and $(\text{NH}_4)_3\text{Ti}(\text{O}_2)\text{F}_5$ (II).

For all structures: Cubic, $Fm\bar{3}m$, $Z = 4$. Experiments were carried out at 296 K with Mo $\text{K}\alpha$ radiation using a Bruker APEXII CCD diffractometer. Absorption was corrected for by multi-scan methods, *SADABS* (Bruker, 2008). H atom parameters were not refined.

	(I)	(II)
Crystal data		
Chemical formula	$(\text{NH}_4)_3\text{HfF}_7$	$(\text{NH}_4)_3\text{Ti}(\text{O}_2)\text{F}_5$
M_f	365.62	229.03
a (Å)	9.3964 (1)	9.2327 (1)
V (Å 3)	829.63 (3)	787.02 (3)
D_x (Mg m $^{-3}$)	2.927	1.933
μ (mm $^{-1}$)	12.645	1.143
Crystal size (mm)	0.25 × 0.23 × 0.22	0.24 × 0.23 × 0.22
Data collection		
T_{\min} , T_{\max}	0.593, 0.750	0.695, 0.749
No. of measured, independent and observed [$I > 2\sigma(I)$] reflections	8194, 293, 293	9680, 190, 190
R_{int}	0.019	0.020
(sin θ/λ) $_{\text{max}}$ (Å $^{-1}$)	1.116	0.961
Refinement		
$R[F^2 > 2\sigma(F^2)]$, $wR(F^2)$, S	0.009, 0.019, 1.19	0.014, 0.0400, 1.032
No. of reflections	293	190
No. of parameters	22	24
$\Delta\rho_{\text{max}}, \Delta\rho_{\text{min}}$ (e Å $^{-3}$)	1.14, -0.66	0.14, -0.33

Computer programs used: *SMART* (Bruker, 1998), *SAINT* (Bruker, 2000), *SHELXTL* (Sheldrick, 2015).

Table 2

Selected distances (Å) and angles (°) for (I) and (II).

$(\text{NH}_4)_3\text{HfF}_7$			
Hf–F1	1.963 (2) × 3	F1–F3	2.912 (4) × 4
Hf–F2	2.032 (5) × 2	F1B–F2	2.374 (6) × 2
Hf–F3	2.151 (5) × 2	F2–F3	2.484 (8) × 2
F1–F1B	2.776 (3) × 2	F3–F3A	2.425 (10)
F1–F2	2.826 (4) × 4		
F1–Hf–F1A	180	F2–Hf–F3	72.8 (2) × 2
F1–Hf–F _{eq}	90 × 10	F3–Hf–F3A	68.6 (3)
F2–Hf–F1B	72.9 (2) × 2		
$(\text{NH}_4)_3\text{Ti}(\text{O}_2)\text{F}_5$			
Ti–O1	1.974 (3) × 2	O1–O1A	1.491 (4)
Ti–F1	1.895 (1) × 3	O1–F2	2.362 (5) × 2
Ti–F2	1.928 (3) × 2	O1–F1B	2.707 (3) × 2
F1–F1A	2.673 (2) × 2	F1A–F1B	2.483 (3)
F1–F2	2.386 (3) × 2	F1A–F2A	2.816 (2) × 2
		F2–F2A	2.611 (4)
F1–Ti–F1A	89.73 (7) × 2	O1–Ti–F1B	88.78 (5) × 2
F1–Ti–F2	77.21 (9) × 2	F1A–Ti–F1B	81.90 (7)
O1–Ti–O1A	44.38 (8)	F1A–Ti–F2A	94.89 (5) × 2
O1–Ti–F2	74.5 (1) × 2	F2–Ti–F2A	85.24 (3)

(the solution pH was adjusted at 7–8 by the addition of ammonia, if necessary). As a result, an abundant yellow-lemon deposition of $(\text{NH}_4)_3\text{Ti}(\text{O}_2)\text{F}_5$ formed consisting of fine octahedral single crystals (~ 10 µm in size). Further slow evaporation of the solution in air resulted in larger bright yellow single crystals suitable for X-ray determination.

2.2. Crystallographic determination

Single-crystal X-ray diffraction data were collected using Bruker KAPPA APEX II and Bruker SMART-1000 CCD

diffractometers equipped with a graphite monochromator (Mo $\text{K}\alpha$ radiation, $\lambda = 0.71073$ Å). Data collections were carried out at 296 K, 0.3° ω -scans were performed in a hemisphere of reciprocal space with an exposure time of 20 s per frame at a crystal–detector distance of 40 mm. Data collection, reduction and refinement of the lattice parameters were performed using the *APEXII* software package (Bruker, 1998, 2000). All the calculations were performed using the *SHELXL/PC* program (Sheldrick, 2015).

The structures were solved by direct methods with an analysis of the electron-density distribution and refined against F^2 by the full-matrix least-squares method with anisotropic approximation. At the first stage, the H atoms of ammonium groups were determined from difference electron-density maps. The H1 atoms around N1 form a tetrahedron with the N–H distances of 0.89 and 0.79 Å for (I)

and (II), respectively, while the H2 atoms around N2 form an octahedron with the N–H distances of 0.92 and 0.83 Å for (I) and (II), respectively. Next, the coordinates of the H atoms were calculated geometrically in accordance with N1 disordering and the real geometry of N_2H_4 , and they were not refined. Information on the structure determinations is summarized in Table 1. Selected bond distances and angles are listed in Table 2. The hydrogen-bond parameters are presented in Table 3.

2.3. Spectroscopic measurements and additional characterization

Mid-IR (400–4000 cm $^{-1}$) spectra were collected in Nujol mull using a Shimadzu FTIR Prestige-21 spectrometer operating at 2 cm $^{-1}$ resolution. The FT-Raman spectra of the compounds were recorded with an RFS 100/S spectrometer. The 1064 nm line of an Nd:YAG laser (130 mW maximum output) was used for excitation of the samples. The spectra were recorded at room temperature. In addition, the IR spectrum of $(\text{NH}_4)_3\text{HfF}_7$ was recorded directly from the pure single crystal using a FT-IR Bruker Vertex 70v spectrometer with the Platinum ATR attachment.

For a description of the vibrational spectra of $(\text{NH}_4)_3\text{HfF}_7$, quantum-chemical calculations of the HfF_7^{3-} anion were performed employing the *GAMESS* software package (Schmidt *et al.*, 1993) within the density functional theory framework (DFT) with exchange–correlation potential B3LYP. The TZVP basis set was used for F atoms and SBKJC basis set for Hf.

Table 3
Hydrogen-bonding geometry (\AA , $^\circ$) in (I) and (II).

$D-\text{H}\cdots A$	$D-\text{H}$	$\text{H}\cdots A$	$D\cdots A$	$D-\text{H}\cdots A$
$(\text{NH}_4)_3\text{HfF}_7$				
N1—H11···F3	0.90	2.04	2.798 (6)	141
N1—H12···F2 ⁱ	0.88	2.25	2.967 (3)	138
N1—H12···F2 ⁱⁱ	0.88	2.11	2.856 (5)	142
N1—H12···F3 ⁱⁱ	0.88	1.85	2.584 (4)	140
N1—H12···F3 ⁱ	0.88	1.99	2.695 (3)	136
N1—H12···F3 ⁱⁱⁱ	0.88	1.89	2.620 (3)	138
N1—H12···F2 ⁱⁱⁱ	0.88	2.20	2.933 (4)	139
N1—H11···F2	0.90	2.32	3.085 (7)	143
N2—H2···F1 ^{iv}	0.91	1.88	2.735 (2)	157
N2—H2···F2 ^{iv}	0.91	1.94	2.820 (6)	164
N2—H2···F3 ^{iv}	0.91	2.30	3.163 (5)	158
N2—H2···F2 ^v	0.91	2.04	2.820 (6)	143
$(\text{NH}_4)_3\text{Ti}(\text{O}_2)\text{F}_5$				
N1—H13···O1 ^{vi}	0.88	2.00	2.721 (2)	138
N1—H14···O1 ^{vii}	0.88	2.00	2.721 (2)	138
N1—H12···F2 ^{viii}	0.88	2.17	2.908 (2)	140
N1—H11···F1	0.87	2.49	3.243 (4)	145
N1—H11···O1 ^{ix}	0.87	2.08	2.838 (4)	145
N1—H12···O1 ^x	0.88	1.84	2.613 (3)	145
N1—H12···F2 ^{xi}	0.88	2.06	2.831 (3)	145
N1—H13···F1 ^{xii}	0.88	2.37	3.102 (2)	140
N2—H2···O1 ^{xiii}	0.89	2.27	3.130 (4)	161
N2—H2···F1 ^{xiii}	0.89	1.87	2.737 (1)	162
N2—H2···F1 ^{xiv}	0.89	1.90	2.737 (1)	156
N2—H2···F2 ^{xv}	0.89	1.96	2.825 (3)	164

Symmetry codes: (i) $x - \frac{1}{2}, y - \frac{1}{2}, z$; (ii) $-x + \frac{1}{2}, -y, -z + \frac{1}{2}$; (iii) $-x + \frac{1}{2}, -y + \frac{1}{2}, -z$; (iv) $x, -y + \frac{1}{2}, -z + \frac{1}{2}$; (v) $x - \frac{1}{2}, -y, -z + \frac{1}{2}$; (vi) $-x + \frac{1}{2}, -z, -y + \frac{1}{2}$; (vii) $-y + \frac{1}{2}, -x + \frac{1}{2}, z; (viii) y, -x + \frac{1}{2}, z + \frac{1}{2}$; (ix) $-z, y, x$; (x) $-x + \frac{1}{2}, -z + \frac{1}{2}, y$; (xi) $x, -y + \frac{1}{2}, z + \frac{1}{2}$; (xii) $-y + \frac{1}{2}, z, -x + \frac{1}{2}$; (xiii) $-x + 1, -y + \frac{1}{2}, -z + \frac{1}{2}$; (xiv) $-x + 1, -y + \frac{1}{2}, z + \frac{1}{2}$; (xv) $-x + 1, y + \frac{1}{2}, -z + \frac{1}{2}$.

The elemental composition of $(\text{NH}_4)_3\text{HfF}_7$ was checked using the X-ray microanalyser JXA-8100 Jeol, Japan (the operating voltage is 20 kV, operating current is 1×10^{-8} A) and energy-dispersive spectrometer INCAx-sight, Oxford (resolution is 137 eV).

3. Results and discussion

3.1. Crystal structures

Both compounds $(\text{NH}_4)_3\text{HfF}_7$ (I) and $(\text{NH}_4)_3\text{Ti}(\text{O}_2)\text{F}_5$ (II) crystallize in the cubic space group $Fm\bar{3}m$. The crystal structure of (I) consists of isolated statistically disordered polyhedra HfF_7 in the form of a pentagonal bipyramid (PB) and two kinds of ammonium groups (Fig. 1). The PB configuration for the related $(\text{NH}_4)_3\text{ZrF}_7$ has been reliably established by Hurst & Taylor (1970) and confirmed by us (Udovenko & Laptash, 2008b). It is this polyhedron that was realised in most monomeric crystal structures of Zr and Hf fluoride complexes reviewed by Davidovich (1998) and Davidovich *et al.* (2013).

The crystal structure of (II) is built from disordered polyhedra $\text{Ti}(\text{O}_2)\text{F}_5^{3-}$ in the form of distorted octahedron with the peroxide group at one of the axial corners and two kinds of ammonium groups (Fig. 2). It should be noted that this structure was determined initially by Stomberg *et al.* (1977) with isolated $\text{Ti}(\text{O}_2)\text{F}_5^{3-}$ in the PB form, and the peroxide

group was placed in the equatorial plane of PB. Then Massa & Pausewang (1978) presented a polyhedron as an octahedron with a peroxide ‘dumbbell’ in the axial position. It can also be represented as a distorted (bevelled) monocapped trigonal prism with an O—O edge.

At the first phase of structural determination it was difficult to isolate the local polyhedral symmetry. Direct methods identified uniquely only the M, N1 and N2 atoms in the $4a$, $8c$ and $4b$ positions in accordance with the elpasolite structure. Their atomic coordinates were refined by the least-squares method (LS) with anisotropic approximation to $R_1 = 0.0626$ and 0.1445 for (I) and (II), respectively. From electron-density syntheses calculated for these atoms, only the F atoms in the $(x, 0, 0)$ position are localized, which corresponds to the MF_6 octahedron that contradicts the chemical composition of the compound. Therefore, electron-density sections in the range of the F1 atom have been constructed (Figs. 3*a* and *c*), which show that two independent additional F (O) atoms surround the Hf and Ti atoms in the $96j$ position (Figs. 3*b* and *d*). The structural refinement with these atoms reduced R_1 to 0.0104 and 0.0281 for (I) and (II), respectively. Three independent F atoms (F1, F2 and F3) in (I) form 12 spatial orientations of

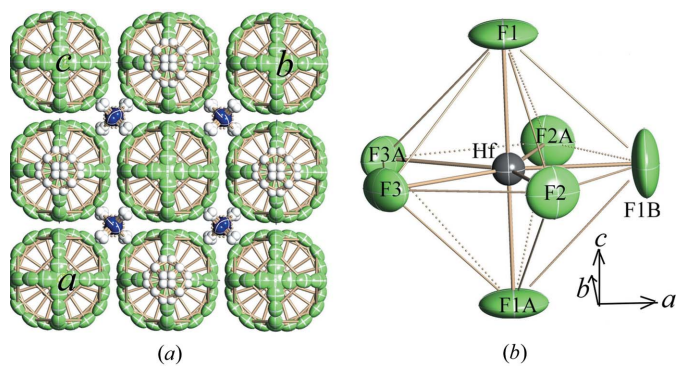


Figure 1
Disordered structure of $(\text{NH}_4)_3\text{HfF}_7$ (a) and the isolated polyhedron HfF_7^{3-} (b). Green, blue and white balls are the F, N and H atoms, respectively (the central Hf atoms are not seen). Displacement ellipsoid plots are shown at 50% probability.

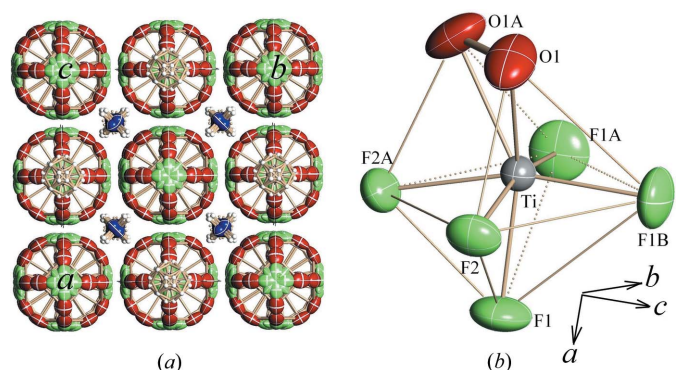
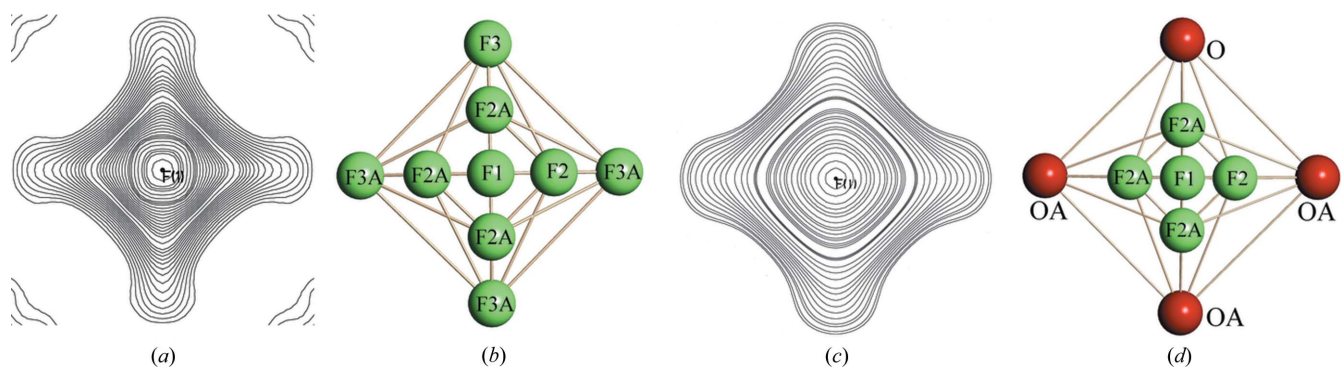
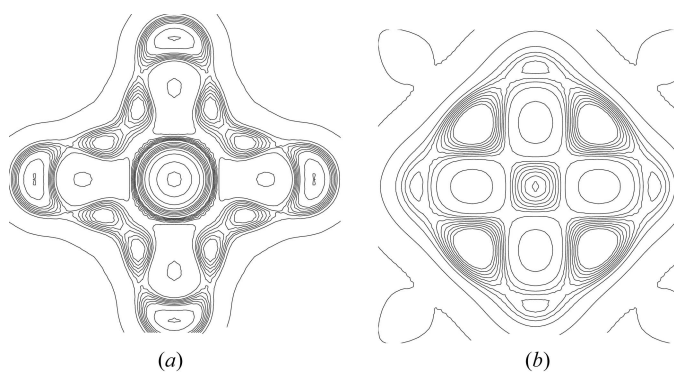


Figure 2
Disordered structure of $(\text{NH}_4)_3\text{Ti}(\text{O}_2)\text{F}_5$ (a) and the isolated polyhedron $\text{Ti}(\text{O}_2)\text{F}_5^{3-}$ (b). Red, blue and white balls are the F, N and H atoms, respectively (the central Ti atoms are not seen). Displacement ellipsoid plots are shown at 50% probability.

**Figure 3**

(a) Electron-density distribution of F1 in $(\text{NH}_4)_3\text{HfF}_7$ on the (001) plane at $z = 0.20$. (b) Arrangement of F1, F2 and F3 atoms on the 24e and 96j positions. (c) Electron-density distribution of F2 in $(\text{NH}_4)_3\text{Ti}(\text{O}_2)\text{F}_5$ on the (001) plane at $z = 0.20$. (d) Arrangement of F1, F2 and O atoms on the 24e and 96j positions.

**Figure 4**

(a) Electron-density distribution of the F1 atom in the (001) plane at $z = 0.20$ of $(\text{NH}_4)_3\text{HfF}_7$. (b) Electron-density distribution of the F1 atom in the (001) plane at $z = 0.20$ of $(\text{NH}_4)_3\text{Ti}(\text{O}_2)\text{F}_5$.

HfF_7 in the PB form (Fig. 1b). Two F atoms (F1 and F2) and one O1 in (II) form 24 orientations of $\text{Ti}(\text{O}_2)\text{F}_5$ in the form of a distorted octahedron (Fig. 2b) with the $(\text{O}_2)^{2-}$ group in the axial vertex.

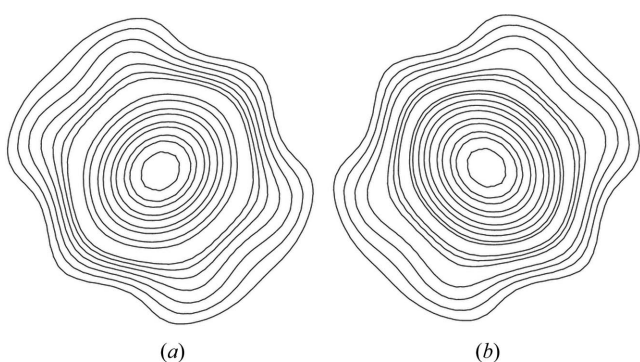
Determined at this stage, our structure of $(\text{NH}_4)_3\text{Ti}(\text{O}_2)\text{F}_5$ was similar to those of $\text{K}_3\text{Ti}(\text{O}_2)\text{F}_5$ (Schmidt & Pausewang, 1986) and $(\text{NH}_4)_3\text{Ti}(\text{O}_2)\text{F}_5$ (Schmidt *et al.*, 1986) with a ‘split-atom’ model. Interestingly, K1 and K2 in the $\text{K}_3\text{Ti}(\text{O}_2)\text{F}_5$

structure were located in the 24e and 32f positions, respectively. However, in all cases two significantly short distances $\text{O}–\text{F}2 = 2.17–2.18 \text{ \AA}$ were present (Fig. 2b). In addition, electron-density synthesis for F1 indicates the 24e position, while Schmidt *et al.* (1986) give the 96k position. The results of structural determination in both cases were very similar, but during several cycles of structural refinement with F1 in the (x, x, z) position the value of x decreased and converged to zero. This is probably owing to the relatively low population of the F1 position and its close surroundings by F2 atoms ($\text{F1}–\text{F2}: 4 \times 0.41 \text{ \AA}$, Fig. 3d). To find the true F1 position, its difference electron-density profiles were built for (I) and (II) for comparison (Fig. 4; F1 was not specified).

The sections show that in the $(\text{NH}_4)_3\text{HfF}_7$ structure F1 occupies the 24e position, while in the $(\text{NH}_4)_3\text{Ti}(\text{O}_2)\text{F}_5$ structure it is placed in the 96k one, but the problem of short O–F distances was not solved. The next step of the structural revision of $(\text{NH}_4)_3\text{Ti}(\text{O}_2)\text{F}_5$ was the change of F1 and F2 populations, wherein two F2 atoms (instead of four) and two F1 atoms were placed in the equatorial octahedral plane. In this case, the structure refinement was successful to $R_1 = 0.0268$ with equalized distances $\text{O}–\text{F}2 = 2.362$ and $\text{F}2–\text{F}1 = 2.386 \text{ \AA}$ instead of 2.183 and 2.623 \AA , respectively, and the F1 coordinates remained in the 96k position.

In accordance with our previous work (Udovenko & Laptash, 2011), where the tetrahedral displacement of N1 from the 8c position was found,

electron-density sections of N1 for (I) and (II) were constructed. Only the sections for (I) are given (Fig. 5), which are very similar to those for (II). The sections show that N1 is displaced from the 8c position. The structure refinement confirmed the escape of N1 from the initial position on 0.14 and 0.15 \AA for (I) and (II), respectively. R_1 changed insignificantly (0.0102 and 0.0256, respectively). The coordinates of H atoms in $\text{N}1\text{H}_4$ were calculated geometrically.

**Figure 5**

Electron-density distribution of N1 in $(\text{NH}_4)_3\text{HfF}_7$ on the (001) plane at $z = 0.20$ (a) and $z = 0.30$ (b). Disorder of tetrahedrally displaced $\text{N}1\text{H}_4$ from the 8c position (c).

Next, the real location of N_2H_4 was found. Two possible models were considered.

Model A: Atom N2 is cubically shifted from the 4*b* position into the 32*f* site, and the H2 atoms occupy the 24*e* position. Taking into account the additional H3 atom in the 32*f* position, the N_2H_4 group forms eight spatial orientations in the structure as was described for the case of $(\text{NH}_4)_3\text{MoO}_3\text{F}_3$ (Udovenko & Laptash, 2008a).

Model B: The N2 atom does not leave the 4*b* position and the H2 atoms are shifted from the 24*e* position into the 96*k* one. Taking into account the additional H3 atom in the 32*f* position, the N_2H_4 group also forms eight spatial orientations.

These two models were not previously supported experimentally. The problem has been solved in the present work owing to the good quality of single crystals and a large set of experimental data. Electron-density sections of N2 for (I) and (II) in the (001) plane with $z = 0.518$ and $z = 0.593$ were constructed. The z coordinate of N2 and H2 was taken from the $(\text{NH}_4)_3\text{MoO}_3\text{F}_3$ structure (Udovenko & Laptash, 2008a) and from the $(\text{NH}_4)_3\text{AlF}_6$ structure (Udovenko & Laptash, 2011), the H atoms were not specified (Fig. 6). The sections for (I) and (II) are similar.

It is seen from Fig. 6 that the outer electron cloud of the N2 atom is deformed by the octahedron, while its internal cloud is spherical which is inconsistent with the N2 escape on the cube from the 4*b* position. The structural refinement with the displaced atom returns it into the initial position and the N2 atom therefore occupies the 4*b* position.

It follows from Figs. 6(a) and (b) that the H2 atoms are statistically distributed in the 96*k* position, and every vertex of the N_2Q_6 octahedron is surrounded by four H2 atoms with a side of the square equal to 0.35 Å. A superposition of electron densities from four H2 atoms in squares forms an octahedral surrounding of the N2 atom by the Q electron-density peaks (Fig. 6c). The final refinement of the structure in the space group $Fm\bar{3}m$ including H atoms reduced the R_1 value to 0.0090 and 0.0140 for (I) and (II), respectively.

Finally, the structural refinements of (I) and (II) were performed in other possible space groups. The results of the refinement of (I) in $Fm\bar{3}m$, $F\bar{4}3m$ and $F432$ were identical, while in $F23$ they became worse [$F_{eq}-F_{eq} = 2.58$ and 2.27 instead of 2.38 and 2.47 (1) Å; $U^{11} = 0.26$ instead of

0.11 (1) Å²]. The refinement of (II) in $F432$ and $F23$ resulted in strong distortion of the $\text{Ti}(\text{O}_2)\text{F}_5$ polyhedron. The refinement in $F43m$ gave the O–F distance 2.20 (1) instead of 2.36 (1) Å for $Fm\bar{3}m$ at the same $R_1 = 0.0140$. Thus, the space group for (I) and (II) is $Fm\bar{3}m$.

$(\text{NH}_4)_3\text{HfF}_7$ is isostructural with $(\text{NH}_4)_3\text{ZrF}_7$ and $(\text{NH}_4)_3\text{NbOF}_6$, the crystal structures of which were described by us previously in the space group $F23$ (Udovenko & Laptash, 2008b), which allowed us to eliminate abnormally short F–F distances (2.16 Å) in the equatorial plane of PB determined by Hurst & Taylor (1970) for $(\text{NH}_4)_3\text{ZrF}_7$ in $Fm\bar{3}m$. Now we repeated the refinement of these structures in both $F23$ and $Fm\bar{3}m$ space groups. The geometrical parameters of the polyhedron NbOF_6 in these two groups are the same within experimental error [$F_{eq}-F_{eq} = 2.36$ (1) and 2.37 (1); 2.41 (1) and 2.41 (1); 2.31 (1) and 2.32 (1) Å for $F23$ and $Fm\bar{3}m$, in pairs, respectively], whereas the parameters of ZrF_7 are appreciably different [$F_{eq}-F_{eq} = 2.47$ (1), 2.50 (1) and 2.36 (1) Å in $F23$ and $F_{eq}-F_{eq} = 2.61$ (1), 2.67 (1) and 2.26 (1) Å in $Fm\bar{3}m$]. The latter geometry is less preferable than the former one due to the shorter F–F contact (2.26 relative to 2.36 Å). Nevertheless, both cubic space groups ($Fm\bar{3}m$ and $F23$) are characteristic of the crystal structure of $(\text{NH}_4)_3\text{ZrF}_7$. The heat capacity (studied by differential scanning microcalorimetry and adiabatic calorimetry), thermal dilation and permittivity investigations revealed the existence of transitions between these two cubic phases (Fokina *et al.*, 2013) near room temperature (290 K). Group theory analysis of PTs has shown that both cubic phases can be transformed into an orthorhombic one ($Imm\bar{m}$) found by polarizing optical studies at $T_1 = 280$ K (Misylu *et al.*, 2008). The crystal structure determination of the latter was unsuccessful because of its complicated twinning structure. The same concerns $(\text{NH}_4)_3\text{HfF}_7$ as our preliminary calorimetric measurements show, different to those for $(\text{NH}_4)_3\text{NbOF}_6$ (Fokina *et al.*, 2007). The refinement of $(\text{NH}_4)_3\text{HfF}_7$ in $F23$ increased the R_1 from 0.0090 to 0.0110, and the F–F equatorial distances were less acceptable [$F-F = 2.274$ (8), 2.419 (6), 2.565 (1) Å instead of 2.374 (6), 2.425 (10), 2.484 (8) Å], and the U^{ii} (U^{11} , U^{22} , U^{33}) parameters of F atoms increased significantly (0.20–0.26 instead of 0.06–0.11 Å²). Therefore, the symmetry of $(\text{NH}_4)_3\text{HfF}_7$ is really $Fm\bar{3}m$, which is the parent phase for both $(\text{NH}_4)_3\text{ZrF}_7$ and $(\text{NH}_4)_3\text{HfF}_7$ compounds.

We also revised the crystal structures of ammonium fluoroelpasolites $(\text{NH}_4)_3\text{ZrF}_7$, $(\text{NH}_4)_3\text{NbOF}_6$, $(\text{NH}_4)_3\text{MoO}_3\text{F}_3$, $(\text{NH}_4)_3\text{WO}_3\text{F}_3$ and $(\text{NH}_4)_3\text{AlF}_6$ with respect to the escape of N1 and N2 from the special 8*c* and 4*b* positions. It is shown that the N1 atom is displaced from the 8*c* position into the 32*f* site and tetrahedrally disordered, while the N2 atom remains in the 4*b* position. The H atoms of N_2H_4 statistically

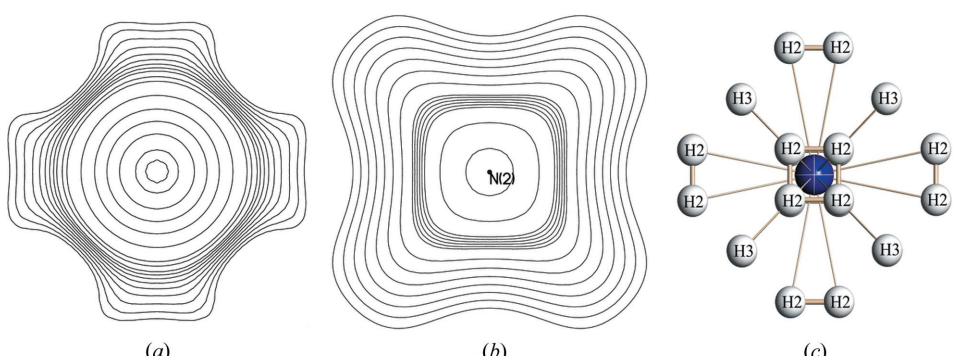


Figure 6

Electron-density distribution of the N2 atom in $(\text{NH}_4)_3\text{Ti}(\text{O}_2)\text{F}_5$ on the (001) plane at $z = 0.518$ (a) and $z = 0.593$ (b). Statistically disordered arrangement of H2 and H3 atoms in N_2H_4 (c).

occupy the $64k$ and $32f$ positions and form eight spatial orientations in the structure.

X-ray crystallographic files in CIF format for the structure determinations of $(\text{NH}_4)_3\text{ZrF}_7$, $(\text{NH}_4)_3\text{NbOF}_6$, $(\text{NH}_4)_3\text{MoO}_3\text{F}_3$, $(\text{NH}_4)_3\text{WO}_3\text{F}_3$ are in the supporting information and can also be obtained from Fachinformationszentrum Karlsruhe, 76344 Eggenstein-Leopoldshafen, Germany [fax: (+49)7247-808-666; e-mail: crystdata@fiz-karlsruhe.de; http://www2.fiz-karlsruhe.de/icsd_home.html] on quoting the

deposition numbers: CSD-431917; CSD-431918; CSD-431919 and CSD-431920, respectively.

3.2. On the $(\text{NH}_4)_3\text{HfOF}_5$ elpasolite

Recently the synthesis and crystal structure of ammonium hafnium oxofluoroelpasolite $(\text{NH}_4)_3\text{HfOF}_5$ was described (Underwood *et al.*, 2013). The compound was prepared hydrothermally from HfF_4 and an aqueous solution of NH_4F at 673–848 K over 3–5 d. Interestingly, $(\text{NH}_4)_3\text{HfOF}_5$ has been observed regardless of the reaction conditions. The crystal structure of this compound was solved classically with ammonium ions being fully ordered at $4b$ and $8c$ sites. The F atom was present at the $24e$ site. When the substitutional model ($5/6$ F and $1/6$ O at the $24e$ site) was used, the R_1 value was 0.0259. The authors attempted to disorder the F and O atoms between the $24e$ site and a $96j$ site in accordance with our mixed ligand position, but their refinements were unsuccessful. The authors also provide the IR spectrum of $(\text{NH}_4)_3\text{HfOF}_5$ (Fig. S3 in their paper), which is identical to that of our $(\text{NH}_4)_3\text{HfF}_7$ recorded from the sample pressed into pellets with KBr or in the Nujol mull. Fig. 7 shows the IR spectrum of a pure single crystal of $(\text{NH}_4)_3\text{HfF}_7$ together with its Raman spectrum. It should be noted that the vibrational spectra of $(\text{NH}_4)_3\text{HfF}_7$ and $(\text{NH}_4)_3\text{ZrF}_7$ (Krylov *et al.*, 2012) are very similar. Spectral lines and their positions agree better with D_{5h} symmetry for an isolated $\text{Hf}(\text{Zr})\text{F}_7^{3-}$ ion, in spite of this symmetry group not being a subgroup of the O_h factor group of the crystal. The optimization of geometric parameters of ZrF_7^{3-} (Voit *et al.*, 2015) resulted in a distorted PB configuration with the C_1 (C_s) symmetry, where the F atoms were displaced from the equatorial plane with one of them shifted most strongly. The axial F atoms are also shifted from the axial position that is consistent with a large amplitude vibration of the F1 atoms in our HfF_7^{3-} (Fig. 1b). This means the non-rigidity of the anion (the F1 atom tends to leave the equatorial plane). Thus, the Raman band at 563 cm^{-1} (Fig. 7) is assigned to a fully symmetric stretch (ν_s) of the HfF_7 PB

(D_{5h} symmetry). Two IR bands at 403 and 466 cm^{-1} are assigned to the asymmetric stretch of Hf–axial fluorines ($\nu_{\text{HfF1}_{\text{ax}} - \nu_{\text{HfF2}_{\text{ax}}}}$) and to asymmetric doubly degenerate Hf–equatorial fluorines [$\nu_{\text{as}}(\text{HfF2}_{\text{eq}} - \nu_{\text{HfF1}_{\text{eq}}})$], respectively, in accordance with DFT calculations. Minor bands at 730 and 1080 cm^{-1} are connected with the presence of the hydroxide ion (OH^-). The first one is a transversal vibration of the proton in the triple system $\text{O}-\text{H}\cdots\text{F}$ with a strong hydrogen bond (HB), the second one is the bending vibration of nonbonding OH^- ($\delta\text{HfO-H}$). Above 1400 cm^{-1} , bending, combinational and stretching vibrations of NH_4 groups

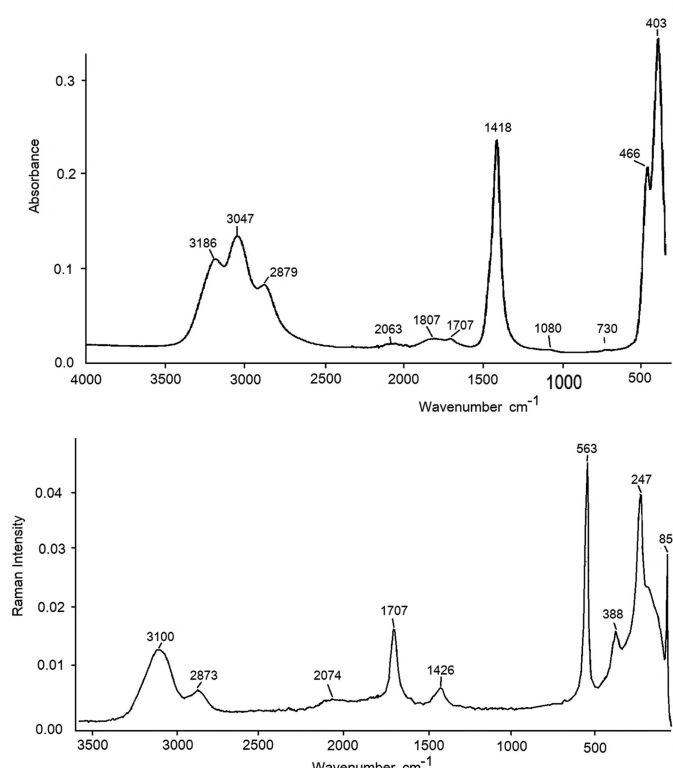


Figure 7
Vibrational spectra of $(\text{NH}_4)_3\text{HfF}_7$ at room temperature: IR – top image, Raman – lower figure.

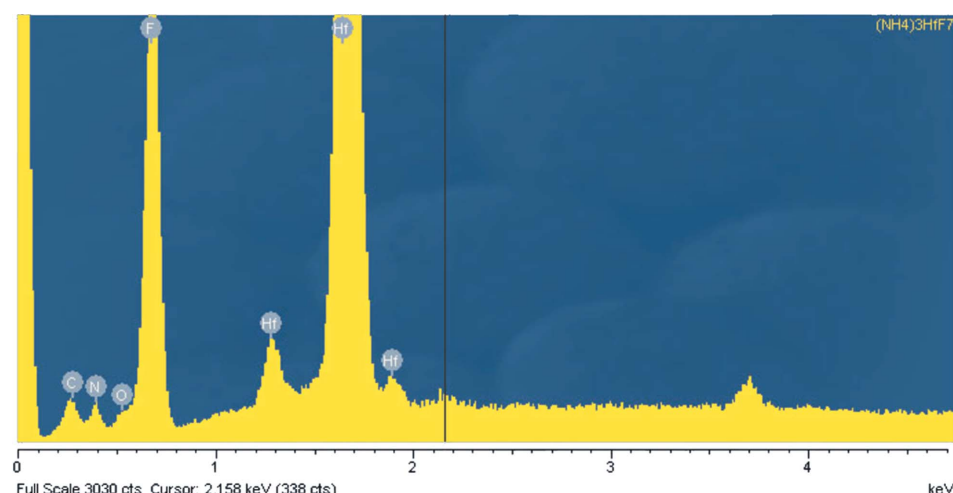


Figure 8
EDX spectrum of $(\text{NH}_4)_3\text{Hf}(\text{OH})_{0.5}\text{F}_{6.7}$.

lie, typical to ammonium elpasolites (Epple *et al.*, 1982). Energy-dispersive X-ray (EDX) analysis corroborates the presence of OH⁻ at the level of 2–4 at. % (Fig. 8), which corresponds to the composition (NH₄)₃Hf(OH)_xF_{7-x} ($x = 0.3$). It is difficult to obtain fluorometallate without the partial substitution of OH⁻ for F⁻.

If the compound composition corresponds to the formula (NH₄)₃HfOF₅, its vibrational spectra should contain the intensive band (both IR and Raman active) in the range 900 cm⁻¹, in accordance with the triple character (one σ + two π) of the Hf—O bond and a short distance of this bond (Gong *et al.*, 2012). Similarly, the Ti—O bond has a triple character (σ + 2 π) that ensures a rather short Ti—O distance in accordance with our structural determinations, and the Ti—O stretches appear at 870 and 897 cm⁻¹ for (NH₄)₃TiOF₅ and Rb₂KTiOF₅, respectively (Udovenko & Laptash, 2011). Thus, the absence of a similar band in the IR spectrum of ammonium hafnium fluoroelpasolite presented by Underwood *et al.* (2013) means that the authors deal with the other compound. According to their elemental analysis (EDX) indicating the presence of oxygen at 6.5–9.1 at. % and fluorine at 51.0–53.6 at %, one can suppose that the real composition of the compound is close to (NH₄)₃Hf(OH)F₆. Our attempts to obtain (NH₄)₃HfOF₅ from solution (by ammonia hydrolysis) were unsuccessful. It seems that is almost impossible. Only zirconium oxofluoroelpasolite with alkali cations A₂BZrOF₅ are known but they were obtained by solid-state reaction: 2AF + BF + ZrOF₂ = A₂BZrOF₅ (A = Cs, Rb, Tl, K; B = Cs, Rb, Tl, K, Na and Li; Verdine *et al.*, 1972). Some of the structures were solved in the classical way.

However, if the compound composition is (NH₄)₃HfOF₅, it would be reasonable to displace a central atom (Hf) from the center of an octahedron towards the O atom to determine the true geometry of the polyhedron. It is possible when the existing disorder has a dynamic nature (Laptash & Udovenko, 2016).

4. Conclusions

Single crystals of (NH₄)₃HfF₇ and (NH₄)₃Ti(O₂)F₅ of high quality were obtained that enabled a large set of experimental data to be collected and the ligand refined with cationic positions in the cubic $F\bar{m}\bar{3}m$ ($Z = 4$) structure with respect to the classic version of the elpasolite structure. All our previously investigated crystal structures of ammonium fluoro- or oxofluoroelpasolites characterized by dynamic orientational disorder were revised in accordance with new features of the fluoroelpasolite structure. The electron-density profiles of all the constituent atoms in the compounds investigated show that the ligand atoms are distributed in a mixed (split) position instead of 24e. One of the ammonium groups is disordered near 8c so that its central atom (N1) forms a tetrahedron with vertexes in 32f, but a center of another group (N2) remains in 4b, whereas its H atoms (H2) occupy the 96k position instead of 24e, and together with the H3 atom in the 32f position they form eight spatial orientations of the ammonium group. On cooling these compounds undergo PTs

of an order-disorder type with a rather large value of entropy changes. These values are rather different [from $Rln3$ for (NH₄)₃Ti(O₂)F₅ to $Rln136$ for (NH₄)₃NbOF₆], but they should be taken into account during the structure refinement to clarify the mechanism of PTs. Easy transformation between two cubic phases ($Fm\bar{3}m$ and $F23$) near the room temperature in the case of (NH₄)₃ZrF₇ and (NH₄)₃HfF₇ is very interesting and deserves further special consideration.

Acknowledgements

We thank T. B. Emelina for DFT calculations of vibrational spectra of (NH₄)₃HfF₇ and Yu. V. Marchenko for recording its IR spectrum.

References

- Bruker (1998). SMART, Version 5.054. Bruker AXS Inc., Madison, Wisconsin, USA.
- Bruker (2000). SAINT, Version 6.02a. Bruker AXS Inc., Madison, Wisconsin, USA.
- Bruker (2008). SADABS. Bruker AXS Inc., Madison, Wisconsin, USA.
- Bučko, T. & Šimko, F. (2016). *J. Chem. Phys.* **144**, 064502.
- Davidovich, R. L. (1998). *Russ. J. Coord. Chem.* **24**, 751–768.
- Davidovich, R. L., Marinin, D. V., Stavila, V. & Whitmire, K. H. (2013). *Coord. Chem. Rev.* **257**, 3074–3088.
- Epple, M., Rüdorff, W. & Massa, W. (1982). *Z. Anorg. Allg. Chem.* **495**, 200–210.
- Flerov, I. N., Gorev, M. V., Aleksandrov, K. S., Tressaud, A. & Fokina, V. D. (2004). *Crystallogr. Rep.* **49**, 100–107.
- Flerov, I. N., Gorev, M. V., Aleksandrov, K. S., Tressaud, A., Grannec, J. & Couzi, M. (1998). *Mater. Sci. Eng. Rep.* **24**, 81–151.
- Flerov, I. N., Gorev, M. V., Grannec, J. & Tressaud, A. (2002). *J. Fluor. Chem.* **116**, 9–14.
- Flerov, I. N., Gorev, M. V., Tressaud, A. & Laptash, N. M. (2011). *Crystallogr. Rep.* **56**, 9–17.
- Fokina, V. D., Flerov, I. N., Gorev, M. V., Bogdanov, E. V., Bovina, A. F. & Laptash, N. M. (2007). *Phys. Solid State*, **49**, 1548–1553.
- Fokina, V. D., Flerov, I. N., Molokeev, M. S., Pogoreltsev, E. I., Bogdanov, E. V., Krylov, A. S., Bovina, A. F., Voronov, V. N. & Laptash, N. M. (2008). *Phys. Solid State*, **50**, 2175–2183.
- Fokina, V. D., Gorev, M. V., Bogdanov, E. V., Pogoreltsev, E. I., Flerov, I. N. & Laptash, N. M. (2013). *J. Fluor. Chem.* **154**, 1–6.
- Gong, Y., Andrews, L., Bauschlicher, C. W. Jr, Thanthiriyawatte, K. S. & Dixon, D. A. (2012). *Dalton Trans.* **41**, 11706–11715.
- Gorev, M. V., Flerov, I. N., Bogdanov, E. V., Voronov, V. N. & Laptash, N. M. (2010). *Phys. Solid State*, **52**, 377–383.
- Hirokawa, K. & Furukawa, Y. (1988). *J. Phys. Chem. Solids*, **49**, 1047–1056.
- Hurst, H. J. & Taylor, J. C. (1970). *Acta Cryst. B* **26**, 417–421.
- Kavun, V. Ya., Gabuda, S. P., Kozlova, S. G., Tkachenko, I. A. & Laptash, N. M. (2011). *J. Fluor. Chem.* **132**, 698–702.
- Kavun, V. Ya., Kozlova, S. G., Laptash, N. M., Tkachenko, I. A. & Gabuda, S. P. (2010). *J. Solid State Chem.* **183**, 2218–2221.
- Kobayashi, K., Matsuo, T., Suga, H., Khairoun, S. & Tressaud, A. (1985). *Solid State Commun.* **53**, 719–722.
- Krahl, T., Ahrens, M., Scholz, G., Heidemann, D. & Kemnitz, E. (2008). *Inorg. Chem.* **47**, 663–670.
- Krylov, A. S., Krylova, S. N., Laptash, N. M. & Vtyurin, A. N. (2012). *Vibr. Spectrosc.* **62**, 258–263.
- Laptash, N. M., Maslennikova, I. G. & Kaidalova, T. A. (1999). *J. Fluor. Chem.* **99**, 133–137.
- Laptash, N. M. & Udovenko, A. A. J. (2016). *J. Struct. Chem.* **57**, 390–398.
- Massa, W. & Babel, D. (1988). *Chem. Rev.* **88**, 275–296.

- Massa, W., Babel, D., Epple, M. & Rüdorff, W. (1986). *Rev. Chim. Miner.* **23**, 508–519.
- Massa, W. & Pausewang, G. (1978). *Mater. Res. Bull.* **13**, 361–368.
- Misyul, S. V., Mel'nikova, S. V., Bovina, A. F. & Laptash, N. M. (2008). *Phys. Solid State*, **50**, 1951–1956.
- Moriya, K., Matsuo, T., Suga, H. & Seki, S. (1977). *Bull. Chem. Soc. Jpn.* **50**, 1920–1926.
- Moriya, K., Matsuo, T., Suga, H. & Seki, S. (1979). *Bull. Chem. Soc. Jpn.* **52**, 3152–3162.
- Morss, L. R. J. (1974). *Inorg. Nucl. Chem.* **36**, 3876–3878.
- Schmidt, M. W., Baldridge, K. K., Boatz, J. A., Elbert, S. T., Gordon, M. S., Jensen, J. H., Koseki, S., Matsunaga, N., Nguyen, K. A., Su, S., Windus, T. L., Dupuis, M. & Montgomery, J. A. (1993). *J. Comput. Chem.* **14**, 1347–1363.
- Schmidt, R. & Pausewang, G. (1986). *Z. Anorg. Allg. Chem.* **537**, 175–188.
- Schmidt, R., Pausewang, G. & Massa, W. (1986). *Z. Anorg. Allg. Chem.* **535**, 135–142.
- Sheldrick, G. M. (2015). *Acta Cryst. C* **71**, 3–8.
- Smrčok, L., Kucharík, M., Tovar, M. & Žižák, I. (2009). *Cryst. Res. Technol.* **44**, 834–840.
- Stomberg, R., Svensson, I.-B., Näsläkkälä, E., Pouchard, M., Hagenmüller, P. & Andresen, A. F. (1977). *Acta Chem. Scand. A*, **31**, 635–637.
- Tressaud, A., Khaïroun, S., Rabardel, L., Kobayashi, T., Matsuo, T. & Suga, H. (1986). *Phys. Status Solidi. A*, **96**, 407–414.
- Udovenko, A. A. & Laptash, N. M. (2008a). *Acta Cryst. B* **64**, 305–311.
- Udovenko, A. A. & Laptash, N. M. (2008b). *J. Struct. Chem.* **49**, 482–488.
- Udovenko, A. A. & Laptash, N. M. (2011). *Acta Cryst. B* **67**, 447–454.
- Udovenko, A. A., Laptash, N. M. & Maslennikova, I. G. (2003). *J. Fluor. Chem.* **124**, 5–15.
- Underwood, C. C., McMillen, C. D., Chen, H. G., Anker, J. N. & Kolis, J. W. (2013). *Inorg. Chem.* **52**, 237–244.
- Vasilovsky, S. G., Sikolenko, V. V., Beskrovny, A. I., Belushkin, A. V., Flerov, I. N., Tressaud, A. & Balagurov, A. M. (2006). *Z. Kristallogr. Suppl.* **2006**, 467–472.
- Verdine, A., Belin, D. & Besse, J.-P. (1972). *Bull. Soc. Chim. Fr.* **1**, 76–78.
- Voit, E. I., Didenko, N. A. & Galkin, K. N. (2015). *Opt. Spectrosc.* **118**, 114–124.
- Yakubovich, O. V., Kiryukhina, G. V. & Dimitrova, O. V. (2013). *Crystallogr. Rep.* **58**, 412–415.
- Yang, H., Ghose, S. & Hatch, D. M. (1993). *Phys. Chem. Miner.* **19**, 528–544.
- Zhou, Q. G. & Kennedy, B. J. (2004). *J. Solid State Chem.* **177**, 654–659.